TIME HISTORY STUDY OF A CLASSICAL CANTILEVER BEAM DAMPED BY INTERNAL MECHANICAL MEANS

C. M. North
Rose-Hulman Institute of Technology
Terre Haute, Indiana USA

and

T. A. Nale
General Motors Corporation
Allison Gas Turbine Division
Indianapolis, Indiana USA

ABSTRACT

The impact damped classical elastic cantilever beam in free decay is studied in its many states of vibration by means of time history studies. The effective damping is correlated with the impact mass behavior. The three major behavior regimes studied are: (1) a high amplitude range with an infinite number of impacts per half cycle resulting in decreased damping effectiveness, (2) a moderate amplitude range with a highly useful finite number of impacts per half cycle resulting in the most effective damping, and (3) a low amplitude range with less than one impact per half cycle yielding very low damping. The relative effects on energy dissipation produced in the beam by variations in the number of natural modes used during calculation, impactor/beam mass ratio, and impactor/beam coefficient of restitution are studied. These parametric studies have shown that the impactor reduces the amplitude of beam vibration in the same fashion regardless of the number of natural modes used during calculation. Furthermore it is shown that the most effective damping occurs when the dimensionless amplitude of transverse beam vibration at the longitudinal cavity coordinate is less than 1.0 independent of all other parameters.

NOMENCLATURE

A	Beam Height
B	Beam Width
C	Cavity Depth
D	Impactor Height
e	Coefficient of Restitution
E	Linear Spring Potential Energy
ΔE	Change in Linear Spring Potential Energy
EI	Beam Flexural Rigidity
E_x	Cavity Width
E_y	Total Cavity Length
e_x	E_x/L - Dimensionless Cavity Width
F_o	Magnitude of Sine Input
f_o	$F_o/\rho V^2$ - Dimensionless Magnitude of Sine Input
F(X)	Initial Beam Displacement
f(x)	F(X)/L - Dimensionless Initial Beam Displacement
G(X)	Initial Beam Velocity
g(x)	G(X)/L - Dimensionless Initial Beam Velocity
H	E_y-D - Cavity Length (Gap)
h	H/L - Dimensionless Cavity Length (Gap)
L	Beam Length
M	Impactor Mass
m	Dimensionless Impactor to Beam Mass Ratio
P_i	Magnitude of Impulse During Impact at $T = T_i$
p_i	$P_i/\rho LV$ - Dimensionless Impulse During Impact
T	Real Time
T_c	Beam Characteristic Wave Time
t	T/T_c - Dimensionless Time
t_i	Dimensionless Time of Impact with Cavity Wall
$\bar{T}_n$	Average Period of Oscillation Across Five Cycles
U(T)	Relative Displacement of Impactor
u(t)	U(T)/H - Dimensionless Impactor Relative Displacement
W(T)	$Y(X_o+0.5E_x,T)$ - Cavity Deflection
w(t)	W(T)/L - Dimensionless Cavity Deflection
X	Beam Longitudinal Coordinate
x	X/L - Dimensionless Beam Longitudinal Coordinate
X_f	Longitudinal Coordinate of Sine Force $X_f = X_o+(0.5)E_x$
x_f	X_f/L - Dimensionless Location of Sine Force
X_o	Longitudinal Coordinate of Cavity Left Wall $0 < X_o < X_o+E_x < L$
x_o	X_o/L - Dimensionless Location of Cavity
y	Linear Spring Deflection
Δy	Change in Linear Spring Deflection
Y(X,T)	Transverse Beam Deflection (Neutral Axis)
y(x,t)	Y(X,T)/L - Dimensionless Transverse Beam Deflection
1(T)	Heaviside Unit Step Function
$\delta(T)$	Dirac Impulse Function
η	Loss Factor for One Half Cycle
ρ	Beam Mass per unit Length
ϕ_i	Phase angle at Impact t_i
Ω	Angular Frequency of Sine Input
ω_f	ΩT_c - Dimensionless Angular Frequency of Sine Input
ω_k	Beam Natural Modal Frequencies

INTRODUCTION

Impact damping dissipates vibrational energy by internal mechanical means. The primary model of the mechanism by which energy is removed from the system is the coefficient of restitution. A simple but effective illustration of how the coefficient of restitution is used to model energy loss during impact is a bouncing ball in a uniform gravitational field. During the bouncing process the maximum height reached during each successive cycle is smaller than that of the previous cycle. For this to be true the energy of the ball, which is the sum of the kinetic and potential energies at any point in time, has decreased by some finite amount. This decrease in the total energy is a function of the decrease in the ball's maximum height between two successive cycles. For the case of a ball bouncing on a hard floor in a constant gravitational field in the absence of air resistance the "coefficient of restitution is simply the square root of the ratio of the maximum height after impact to the maximum height before impact"[1]. It can be easily shown that the ball's rebound height becomes successively smaller while approaching zero. Although the ball will theoretically go through an infinite number of bounces, this occurs in a finite period of time. For practical purposes the ball is said to be resting on the floor at the end of this finite time. This phenomenon is referred to herein as "bounce-down". It will be shown later that the damping effectiveness of an impact damped system depends heavily upon the amplitude of oscillation at the cavity.

The history of impact damping can be traced to 1833 in published literature. Although this subject has a long history it appears that the majority of recently published work has been done by Masri[2], Bapat and Popplewell[3]. Past work done in the area of impact damping has concentrated on the analysis of steady-state forced oscillators. In doing this the authors have assumed a steady-state solution, generally two impacts per half cycle. These assumed solutions limit the impactor analysis to a narrow range of cavity amplitudes. The use of these limited solutions does give the reader an indication of the effectiveness of impact dampers but is inadequate for determining the optimum damper effectiveness.

In 1982, under sponsorship of NASA Lewis Research Center, Brown and North[4] initiated the study of the transient response of the simple harmonic oscillator with a single internal impact damper. These studies began with the development of an analytical and a digital computer model of an undamped, freely vibrating simple harmonic oscillator having a single cavity containing a single frictionless impact damper. A second model that was developed by North (unpublished) included the effects of Coulomb friction between the impactor and the primary mass. In 1986 the authors began to develop a digital model of the free and forced vibration of a classical elastic cantilever beam damped by a single internal frictionless impact damper. The results obtained from the beam model are the subject of this document.

The study of a continuous beam subject to impact damping in free decay may appear to be unimportant compared to the study of impact damping of the forced beam. This is not necessarily so. Analysis of the transient free decay of the impact damped beam provides a great deal of valuable information which can be applied to the forced vibrating beam with impact damping.

First, there exist several characteristics of transient free decay which also apply to forced response. It is later shown that impact damping is

frequency independent. This leads to the conclusion that impact damping effectiveness is independent of a forcing function's frequency. Impact damping is found to be most heavily dependent upon the amplitude of vibration experienced by the beam cavity. Free decay initial cavity amplitudes are used to span a wide range of forcing functions magnitudes. This allows free decay analysis to be applied to forced motion response of various transient and steady state cavity amplitudes.

Secondly, the simplicity of free motion makes it more advantageous to study than forced motion response. The absence of large transient conditions during free decay make it possible to observe the several impactor behavioral characteristics within shorter time intervals than would be required for transient forced motion. Free decay characterizes impact damping across a wide range of beam cavity vibrational amplitudes using a single time-history profile with appropriately chosen initial conditions. The patterned behavior which characterizes impactor motion is more easily discerned with the use of free decay time histories. The presence of a forcing function can eliminate a significant portion of the impactor's patterned spectrum.

Finally, the study of transient free decay can be made to simulate the recovery from the occurrence of a transient disturbance to a steady state beam[4]. All of these reasons make the use of transient free decay time-history studies useful.

The application of impact damping would provide a means of significantly decreasing the amplitude of vibration without altering the external configuration of the system. The use of impact dampers also could reduce the fatigue effects of vibration experienced by aerospace parts. This would allow the stringency of design criteria for such parts to be relaxed. The reduced effects of fatigue would allow lighter weight parts with a longer working lifetime to be produced.

This study was initiated to determine the characteristics and effectiveness of impact damping applied to a continuous elastic cantilever beam. The overall motivating factor for these studies is a desire to investigate the concept of adding very light damping to aerospace systems which exhibit self-excited vibration or forced vibration near a natural frequency. This research was performed with the following objectives in hand:

1.) Compare the effects of impact damping applied to continuous elastic cantilever beams with that of simple harmonic oscillators. Determine the similarities and differences in the behavior of the two applications.

2.) Determine the effects of higher modal frequencies on the characteristic behavior of the impactor and the ability of impact damping to effectively reduce continuous elastic cantilever beam vibration amplitude.

3.) Evaluate the ability of impact dampers to inhibit vibration. This decrease in vibration amplitude is quantified by means of loss factor evaluation.

4.) Determine impactor behavior and damping effectiveness as the cavity vibrational amplitude decays.

5.) Measure the change in effective damping with respect to variations in the impactor/beam mass ratio.

6.) Evaluate the effects of the coefficient of restitution on the characteristic behavior and damping effectiveness of the impactor.

IMPACTOR BEHAVIOR AND DECAY STUDY

A FORTRAN digital model of the impact damped classical elastic cantilever beam, Figures 1 and 2, was developed for the purpose of performing parametric studies of beam impactor performance. The longitudinal position of the beam cavity, x_o, is set at 0.684 units. This cavity location was determined by use of beam mode shape displacement analysis. This cavity position is used to maximize the vibrational activity of the beam at the location of the impactor[5]. During this study the initial conditions of the beam were such that the first mode was excited with an initial generalized displacement of 0.05 and no initial generalized velocity. The magnitude of the resulting initial dimensionless displacement of the cavity was 6.0 units. The effects of varying the initial conditions are not explored in this study. Mass ratios of 1.0, 2.0, and 3.0 percent and coefficients of restitution of 0.5, 0.6, 0.7, and 0.8 were used to generate the time histories. The geometrical configuration of the beam is kept unchanged for the time history studies discussed in this report. The magnitudes of the dimensionless physical beam dimensions were determined by a comparative analysis with the data used by Brown and North[4]. A cavity width, e_x, of 0.04 units and a cavity length, h, of 0.01 units are used, Figures 1 and 2. The beam is unforced with no initial relative displacement or relative velocity of the impactor. Another parameter that is varied in this study is the number of mode shapes used during computation. Time histories were made with 1, 2, 5, and 10 mode shapes for the varying mass ratios with a constant coefficient of restitution of 0.6. From this comparative analysis it was found that the higher modal frequencies are of little significance when determining the damping effectiveness of the impactor.

The impactor relative displacement and absolute displacement curves presented in the Appendix, Figures 3 thru 7, show how the impactor behaves as the cavity amplitude of vibration decays. Note that in Figures 6 and 7 the solid lines represent the top and bottom cavity walls with the dashed line representing the impactor. At first, during high amplitude motion, Figure 3, the impactor experiences an infinite number of impacts per half cycle. This occurs because the cavity wall is moving in the same direction as the impactor with a velocity of greater magnitude than that of the impactor. This type of impactor behavior is referred to as bounce-down and is followed immediately by stuck impactor failure. During bounce-down and stuck impactor failure the impactor exhibits a low level of damping effectiveness. This type of high cavity amplitude impactor behavior ceases at moderate amplitudes and is immediately followed by a range during which a finite number of impacts per half cycle occur. This can be observed in two predominate patterns, the first being an equal number of impacts on each side of the cavity for successive half cycles with the second type of motion being an alternating pattern of even to odd numbers of impacts on opposite cavity walls for successive half cycles. The effectiveness of impact damping steadily increases during this behavior to a maximum damping effectiveness when one impact per half cycle is the pattern of motion, Figures 5 and 6. The damping effectiveness of this

motion is attributed to the fact that the impactor is striking an advancing cavity wall resulting in the most effective reduction of beam velocity experienced as a result of impact damping. When one impact per half cycle is occurring impact damper failure soon follows. When the cyclic motion of the impactor degenerates to occasional random impacts along the cavity wall with less than one impact per half cycle for successive periods, Figure 7, impact damping is no longer effective. Once this occurs the damping of the impactor quickly diminishes.

The presence of higher modes does not alter the basic types of behavior the impactor experiences. However, higher modal frequencies do cause the presence of bounce-down and stuck impactor failure to be less predominate at high amplitudes. As a result the impactor experiences a finite number of impacts per half cycle over a wider cavity amplitude range.

The amplitude decay for the impact damped classical elastic cantilever beam is a simple and quick indicator of the damping occurring as a result of the impactor. The amplitude decay is determined by plotting the amplitude of beam cavity vibration for each half cycle versus the corresponding dimensionless time at which the amplitude occurs (see Figures 8 thru 10).

The effects of the higher mode shapes on the amplitude decay curves are minimal. It is demonstrated in Figure 8 that the amplitude decay for 1, 2, 5, and 10 modes all follow the same general trend with a small increase in the range of time during which low damping effectiveness occurs. This extension of the upper portion of the curve results in the effective regime of behavior to be shifted to a later period in time. Another effect of the higher modes is to cause impact failure to occur at a slightly higher amplitude. Although the point at which impact failure occurs is very important when designing an impact damped system, the higher mode shapes do not significantly change the results from those observed in the single mode case.

The amplitude decay curves for mass ratios of 1, 2, and 3 percent are presented collectively in Figure 9. From this figure the observation can be made that increasing the mass ratio decreases the period of time during which damping of low effectiveness occurs.

The amplitude decay curves for varying values of the coefficient of restitution ranging from 0.5 to 0.8 are shown in Figure 10. From this graph it can be seen that lower values of the coefficient of restitution reduce the time required for equivalent damping. It can also be seen that the decrease in the time required for equivalent damping is not linearly related to the decrease in the coefficient of restitution. As the coefficient of restitution becomes smaller (less than 0.6) the decrease in the time required for equivalent damping becomes significantly less.

LOSS FACTOR RESULTS

The loss factor is defined as the change in beam energy with respect to initial beam energy over a cycle of beam vibration. It can be shown that the loss factor is simply a function of the change in beam cavity amplitude over a cycle of beam vibration with respect to the initial amplitude of the cycle. Applying this fact the calculation of the loss factor was performed using a least squares parabolic fit. This fit is performed to smooth the loss factor

curve and calculate an averaged loss factor, which will be referred to as the loss factor (see Appendix B). The loss factor is plotted with reference to the cavity amplitude. By observing the amplitude decay curve, Figure 8, one would expect the loss factor to increase as the amplitude decreases to the point of impact damper failure. Figure 12 does indeed show this to be the case with impact failure occurring in an amplitude range of 0.3 to 0.07. From this figure it is also observed that the most effective damping which the beam experiences occurs in a cavity amplitude range less than unity. From phase plot Figure 17 whose construction is detailed later, it is illustrated that chaotic and one impact per half cycle behavior of the impactor occurs at amplitudes less than and equal to unity while two impacts per half cycle are experienced by the impactor at an amplitude slightly greater than unity. From this it is concluded that the most effective damping correlates to impactor behavior beginning at the transition from two to one impacts per half cycle.

As previously discussed the influence of higher modes does not play a major factor in changing the behavior of the impact damped classical elastic cantilever beam. This fact is again illustrated by observing the loss factor curves for 1, 2, 5, and 10 modes with all other variables held constant. Figure 11 shows that the presence of higher mode frequencies does not significantly alter the loss factor curve with respect to the cavity amplitude. The presence of higher modal frequencies does tend to band the loss factor about those results obtained for the single mode case. The center of this band width occurs about the first mode. It is therefore concluded that the effects of other parameters on the loss factor can be based upon a first mode comparative analysis.

The impactor to beam mass ratio plays a significant role in determining the value of the loss factor for any given cavity amplitude. More specifically, as seen in Figure 12, increasing the mass ratio results in an increase in the loss factor for all amplitudes prior to impact failure. It is also observed that this increase is a constant value change which can be directly expressed as a function of the reciprocal of the mass ratio. To illustrate this fact the loss factor is divided by the mass ratio to obtain the specific total loss factor. Figure 13 shows that the specific total loss factor reduces all mass dependent loss factors to one common curve as a function of cavity amplitude. The specific total loss factor begins with a magnitude of 0.09 at a cavity amplitude of 6.0 while undergoing stuck impactor behavior and reaches a peak value of 9.0 prior to impact damper failure. From the Mass Normalized Loss Factor plot, Figure 13, it is observed that the specific total loss factor behaves as a linear function of the cavity amplitude with a slope of approximately negative one. To show the extent to which this is true the product of the specific total loss factor and cavity amplitude is illustrated in Figure 14. When observing this result it can be inferred that this product behaves on the average as a constant of magnitude approximately 0.4 for all cavity amplitudes. This constant value interpretation is valid within an error range of ± 25 percent prior to impact damper failure. A significant point of interest is that the simple harmonic oscillator was found to behave in a very similar manner with reference to the loss factor's dependence upon the mass ratio and cavity amplitude[4].

A third parameter which plays a major role in the evaluation of impact damper performance is the coefficient of restitution denoted by e. It is observed that any increase in the coefficient of restitution results in a

decrease in the effectiveness of the impact damper. Another conclusion that can be made is that this decrease in the loss factor is not linearly related to the coefficient of restitution. To effectively amplify changes in the loss factor curve for varying values of the coefficient of restitution the product of the specific total loss factor and cavity amplitude is used to generate the Amplitude Specific Loss Factor curve, Figure 15. From these results it can be more clearly observed that the loss factor is not linearly related to the coefficient of restitution for all cavity amplitudes. Applying a relationship developed by Brown and North[4] the quotient of the amplitude specific loss factor and (1-e) results in Figure 16. This result is valid only within the range of motion for which a finite number of impacts occurs during each half cycle. As with the amplitude specific loss factor this curve can be reasonably approximated as a constant of value 1.0 to within an error of $\pm$30 percent. This illustrates that the loss factor for the classical elastic cantilever beam and simple harmonic oscillator investigated by Brown and North[4] behave in a similar manner with regard to variations in the coefficient of restitution.

IMPACT PHASE

From the beam's initial amplitude of vibratory motion to the point at which impact damper failure occurs there exist several time spans of distinct motion which the impactor experiences. These types of behavior can be observed by calculating the phase angle for each impact across a half cycle of vibration (see Appendix C). Plotting this phase angle in the range from 0^{o} to 180^{o} as a function of the cavity amplitude of vibration yields distinct and well defined patterns and trends for the impactor. These patterns for the one mode case are illustrated in Figure 17. Each impact is denoted by a point marker on these figures. Phase plots are read from bottom to top while progressing from right to left as time increases and amplitude decreases. By reading this graph the number of impacts per half cycle can be determined for any given amplitude. For the case of higher amplitudes the phase plot depicts an infinite number of impacts for a given amplitude. This fact can be observed by noticing that the point markers, representative of each impact, meld into a solid line. When amplitudes diminish below the bounce-down and stuck impactor failure range it is clear that well defined periodic motion of the impactor is occurring. This periodic motion takes one of two forms. The first is a pattern exhibiting an even number of impacts per half cycle while the second contains an odd number of impacts. From this well defined periodic motion the impactor motion degenerates into what is referred to as chaotic motion. This is a type of motion during which no discernible pattern can be extracted. Each zone of chaotic motion then flows into two clear paths know as period doubling. These two paths soon merge into one solid line during which well defined periodic motion of one less order occurs. The combined use of phase plot Figure 17 and loss factor Figure 12 leads to the conclusion that the effectiveness of the impactor increases as the number of impacts per half cycle decreases prior to impact damper failure.

In the case of the phase plot, Figures 18 and 19, the higher mode shapes do play a significant factor in the analysis of impactor behavior. The presence of higher modal frequency vibration disrupts the well ordered motion that is observed in the simple harmonic oscillator and one mode classical elastic cantilever beam case; Figure 17. The presence of higher frequencies

also disrupts the phenomenon of stuck impactor failure. In place of stuck impactor failure the impactor experiences low relative displacement impacting or high intensity bounce-down. In the event the impactor does become stuck it is quickly slung free by the presence of high frequency vibration. While the higher mode frequencies do disrupt the ordered behavior of the impactor it can be seen that significantly fewer impacts per half cycle occur at lower cavity amplitudes.

This study, like that of Brown and North[4], found that variations in the mass ratio affected the phase plots only by increasing and decreasing the number of impacts that occur in a set time frame for the case of one mode. It is observed that smaller mass ratios yield more dense plots because of the increased number of impacts which occur during a incremental decrease in beam cavity amplitude. From this it is concluded that a decrease in the impactor to beam mass ratio increases the number of impacts required to lower the beam cavity vibrational amplitude by a constant value. This implies that the individual effectiveness of each impact is reduced as the mass ratio is lowered. Another point of significance is that variations in the mass ratio do not affect the amplitudes or phase angles for which each distinct pattern of motion occurs. In the presence of higher mode frequencies the phase plots differ as a result of varying the mass ratio but in no discernible pattern.

Unlike the mass ratio, variations in the coefficient of restitution, e, do have a major affect on the phase plot. This analysis shows that while lower values of the coefficient of restitution result in higher loss factors, Figure 15, lower coefficients of restitution also cause bounce-down and stuck impactor failure to occur at much lower amplitudes; Figures 20 and 21. An example of this is a value of the coefficient of restitution equal to 0.5 for which stuck impactor failure occurs at an amplitude as low as 3.0. In comparison a value for the coefficient of restitution of 0.6 results in the termination of stuck impactor failure at an amplitude of 5.0. As previously discussed lowering the value of the coefficient of restitution becomes less effective in decreasing the time required to damp the continuous elastic cantilever beam vibration oscillation to a given amplitude when the coefficient of restitution is less than 0.5. The use of phase plot Figure 20 may help to explain this phenomenon by noting that lowering the value of the coefficient of restitution decreases the amplitude at which stuck impactor failure ceases. This in turn narrows the amplitude range during which efficient damping occurs. This results in a trade off between the energy dissipative properties of the coefficient of restitution and the lower efficiency damping of bounce-down and stuck impactor failure.

CONCLUSIONS

1. The impactor behavior for an impact damped continuous elastic cantilever beam is characteristically the same as that of an impact damped simple harmonic oscillator.

2. The magnitude of the damping effectiveness for an impact damped continuous elastic cantilever beam behaves similarly to the damping effectiveness of a simple harmonic oscillator.

3. The most effective damping of the continuous elastic cantilever beam and simple harmonic oscillator occurs when the cavity vibrational amplitude is less than unity. With the use of phase plots it is shown that this corresponds to impactor motion of less than 2 impacts per half cycle.

4. The presence of higher mode frequencies does not change the damping effectiveness of the impactor. This leads to the conclusion that the first modal frequency predominates impactor damping effectiveness.

5. The loss factor is directly related to the mass ratio. A specific loss factor can be determined by dividing the loss factor by the mass ratio. This results in a single specific loss factor curve with respect to the cavity vibrational amplitude.

6. The loss factor is a function of 1/(1-e) during periodic motion with a finite number of impacts occurring per half cycle. Dividing the specific loss factor by (1-e) yields a single curve with respect to the cavity amplitude with the exception of the bounce-down followed by stuck impactor failure and total impact damper failure.

7. The loss factor can be expressed as a constant of magnitude 1.0. It is shown that the product of the loss factor and cavity amplitude divided by the product of the mass ratio and (1-e) is reasonably constant.

8. For the case of one mode clear patterns of impactor motion can be observed from the phase plot. This motion begins with bounce-down followed by stuck impactor failure at high cavity amplitudes. This degenerates to periodic motion with a distinct finite number of impacts per half cycle at moderate cavity amplitudes. This periodic motion is characterized by chaotic motion and period doubling. Impactor motion of one impact per half cycle is soon followed by impact damper failure. This occurs at low cavity amplitudes when the impactor experiences less than one impact per half cycle.

9. The presence of higher modal frequencies disrupts the regularity of impactor motion.

10. The time scale of the amplitude decay curve is directly related to the mass ratio. Cavity amplitude plotted with respect to the product of the mass ratio and dimensionless time results in a single curve.

11. While the impact damper does not require frequency tuning it does require amplitude tuning. This is the result of the fact that impact damping effectiveness is a function of the cavity's vibrational amplitude.

REFERENCES

[1] Soller, Peter J.,"The Development of a Computer Model as an Aid to the Solution of the Problem of Impact Damping", M.S. Thesis, Rose Hulman Institute of Technology, Terre Haute, IN, 1985.

[2] Masri, S.F., "Analytical and experimental Studies of Impact Dampers", Ph.D. Thesis, California Institute of Technology, Pasadena, CA, (CIT Dynamics Laboratory Report), 1965.

[3] Bapat, C.N., N. Popplewell, and K. McLachlan, "Stable Periodic Motions of an Impact-Pair", Journal of Sound and Vibration, 1983, Volume 87, Number 1.

[4] Brown, Gerald V. and C. Mallory North, "The Impact Damped Harmonic Oscillator in Free Decay", NASA Technical Memorandum 89897, Lewis Research Center, 1987.

[5] Nale, Timothy A.,"Time History Study of a Classical Cantilever Beam Damped by Internal Mechanical Means", M.S. Thesis, Rose Hulman Institute of Technology, Terre Haute, IN, 1988.

APPENDIX A - SYSTEM MATHEMATICAL MODEL

A continuous beam with frictionless impact damping is represented by Figures 1 and 2. A detailed derivation of the equations of motion which model this system are presented by Nale[5]. Figures 1 and 2 are representative of the physical system in dimensional variable form. For this study and the benefit of future studies the system is made dimensionless in the following manner. The beam length, L, is the unit of length with the exception of the impactor relative displacement. The cavity length, $H = E_y - D$, is used as the unit of length for the dimensionless analysis of the relative displacement. The unit of time is the beam characteristic wave time, T_c. The beam mass is used as the unit mass. The equation of motion of the beam is

$$EI\frac{\partial^4 Y}{\partial X^4} + \frac{\partial^2 Y}{\partial T^2} = F_o \exp(i\Omega T)\, 1(T)\, \delta(X - X_f) + \frac{1}{E_x}\left[1(X-X_o) - 1(X-X_o-E_x)\right] \sum_{i=1}^{n} P_i \delta(T - T_i) \qquad (A.1)$$

with boundary conditions given by

$$Y(0,T) = \frac{\partial Y}{\partial X}(0,T) = \frac{\partial^2 Y}{\partial X^2}(L,T) = \frac{\partial^3 Y}{\partial X^3}(L,T) = 0 \qquad T > 0$$

and initial conditions given by:

$$Y(X,0) = F(X) \qquad \text{and} \qquad \frac{\partial Y}{\partial T}(X,0) = G(X) \qquad 0 \le X \le L$$

The equation of motion (A.1) which models the physical system shown in Figures 1 and 2 is made dimensionless with respect to the appropriate unit variables in equation (A.2). Dimensionless variables in (A.2) are denoted by lower case letters corresponding to upper case diminsional variables in (A.1).

$$\frac{\partial^4 y}{\partial x^4} + \frac{\partial^2 y}{\partial t^2} = f_o \exp(i\omega_f t)\, 1(t)\, \delta(x - x_f) + g_o(x) \sum_{i=1}^{n} p_i \delta(t - t_i) \qquad (A.2)$$

where: $$g_o(x) = \frac{1}{e_x}\left[1(x-x_o) - 1(x-x_o-e_x)\right]$$

Boundary conditions:

$$y(0,t) = y'(0,t) = y''(1,t) = y'''(1,t) \qquad t > 0$$

Initial conditions:

$$y(x,0) = f(x) \qquad \text{and} \qquad \dot{y}(x,0) = g(x) \qquad 0 \le x \le 1$$

The impactor motion of the impact damped classical elastic cantilever beam is characterized by four distinct types of behavior. Each of these types of motion are individually modeled by an appropriate set of equations. Once the type of behavior that is occurring is determined the correct model is used to calculate the position, velocity, and acceleration of the impactor and beam at the next point in time.

The simplest case of impactor behavior is impactor free motion (impactor not at the cavity wall). During this period of motion the beam and impactor are totally independent of one another. The beam is modeled as a simple classical elastic cantilever beam having a single sinusoidal point load located any where along the beam length with the exception of the center of the beam cavity. The equation of motion for the beam is solved using the method of generalized displacements (see Nale[5]). The generalized displacements, velocities, and accelerations are determined using the method of LaPlace transforms. The resulting Fourier solutions for beam displacements, velocities, and accelerations are valid until the next impact is experienced.

The impactor in free motion is modeled as a free particle in rectilinear motion. The constant velocity with which the impactor travels is determined at the time of the most recent previous contact with the beam cavity wall.

When the position of the impactor coincides with that of the beam cavity wall an impact or collision of the beam cavity wall and impactor occurs. The impact is modeled by applying the coefficient of restitution theory. The relative velocity $\dot{u}_i$ between the impactor and the beam immediately prior to impact is related to that immediately after impact $\dot{u}_i'$ by:

$$\dot{u}_i' = -e\dot{u}_i \qquad (A.3)$$

The time at which impact occurs is determined when the absolute displacement of the beam cavity wall is equal to that of the impactor. While this time of impact is modeled as instantaneous, the resulting impulse applied to the beam occurs across a finite nonzero cavity width.

A more difficult type of motion to model is that of bounce-down. Motion of this nature is experienced by the system when consecutive impacts on the same cavity wall occur with consistently shorter time intervals between impact. This results in smaller maximum relative displacements between the impactor and cavity wall for consecutive impacts. While experiencing this type of motion an infinite number of impacts occur during a finite period of time. The finite time during which bounce-down occurs is readily determined by means of a convergent geometric series expansion (see Nale[5]). Bounce-down terminates with the impactor resting at the cavity wall for until the acceleration of the cavity wall reverses direction. This occurrence is referred to as "stuck impactor failure".

The impactor is said to be stuck at the cavity wall when the following three conditions occur simultaneously. First, the impactor must be located at the cavity wall. Second, the velocity of the impactor relative to the beam must be zero. Finally, the beam must be accelerating toward the impactor.

During stuck impactor failure the total energy of the freely vibrating impact damped classical elastic cantilever beam system remains constant. At the same time energy is being exchanged between the impactor and beam. This energy transfer process from the beam to the impactor during stuck impactor failure explains why minimal damping occurs even when the impactor is stuck at the beam cavity wall.

While the impactor is stuck there exists a normal reaction between the impactor and the cavity wall. This normal reaction is a direct function of the cavity acceleration. The impactor is slung free of the beam cavity wall and set back in free motion when the normal reaction vanishes. The normal reaction between the impactor and cavity wall is eliminated only when the beam cavity acceleration changes direction.

These four states of impactor activity are used to determine the appropriate set of equations to be used in calculating the position, velocity, and acceleration of the impactor and beam for each progressive point in time. Free motion and simple impact are modeled with relative ease. Bounce-down and stuck impactor failure are more difficult, but not intractable (see Nale[5]).

APPENDIX B - LOSS FACTOR

The loss factor is first illustrated for the simple harmonic oscillator. The results are later applied to the beam model. The loss factor is defined as the change in potential energy E with respect to itself. This relationship is expressed in its most general form as shown in Equation (B.1):

$$\eta = \frac{\Delta E}{E} \tag{B.1}$$

For the case of the simple harmonic oscillator the potential energy, $E = ky^2/2$, is simply the potential energy of the linear spring. The derivative of the spring energy with respect to the spring deflection, y, is used to approximate the change in energy, $\Delta E = ky\Delta y$. Using the expressions for E and ΔE for the simple harmonic oscillator in the general expression (B.1) the loss factor is expressed simply as a function of spring amplitude of vibration:

$$\eta = 2\Delta y/y \quad \text{per cycle} \tag{B.2}$$

The loss factor is in practice calculated using an averaging process by means of a least squares parabolic fit about five full cycles of motion. The change in amplitude, Δy, is expressed as a function of the time rate of change of the amplitude and the average period of oscillation. For this study the loss factor is expressed in dimensionless form. This is done by dividing the loss factor per cycle by 2π resulting in a loss factor per radian. Substitution of the change in amplitude results in Equation (B.3).

$$\eta = \frac{1}{\pi} \frac{\dot{y}(t_n)}{y(t_n)} \bar{T}_n \quad \text{per radian} \tag{B.3}$$

The loss factor for the impact damped classical elastic cantilever beam is determined in a similar manner from (B.3) by using the beam cavity amplitude of vibration in place of the spring deflection y used for the simple harmonic oscillator. This substitution results in a loss factor for the impact damped cantilever beam at the center of the cavity longitudinal coordinate.

APPENDIX C - PHASE ANGLE CALCULATION

The phase angle is used to determine where the impactor collides with the sinusoidal oscillating cavity wall. This measure is made in degrees across each half cycle from 0^{o} to 180^{o}. The phase angle ϕ_i for the impact which occurs at time t_i is easily calculated using Equation (C.1).

$$\phi_i = 180^{o} (t_i - t_n)/(t_{n+1} - t_n) \qquad (C.1)$$

The times, t_n and t_{n+1}, are representative of when the acceleration of the cavity wall changes direction sign.

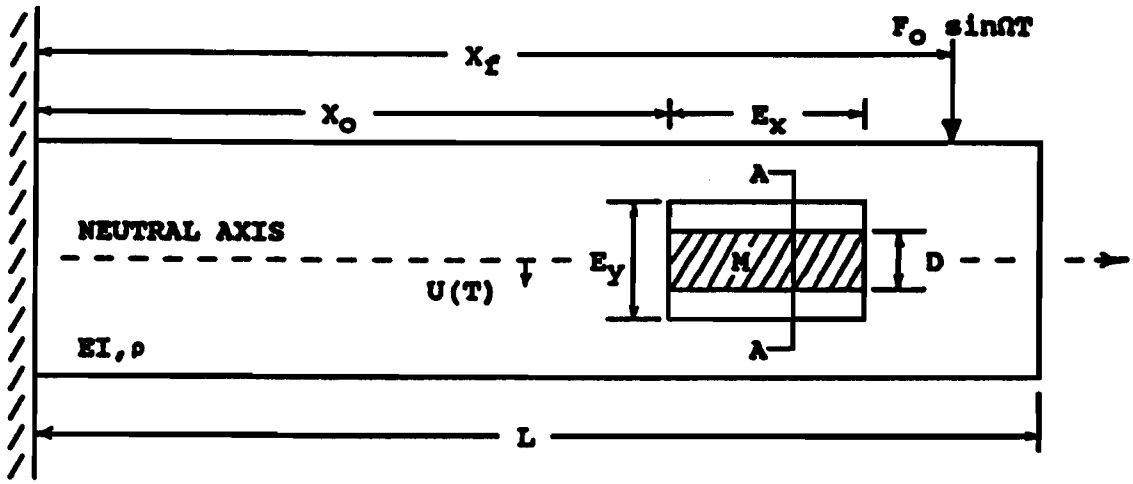

FIGURE 1 - SIDE VIEW SCHEMATIC OF IMPACT DAMPED CLASSICAL ELASTIC CANTILEVER BEAM.

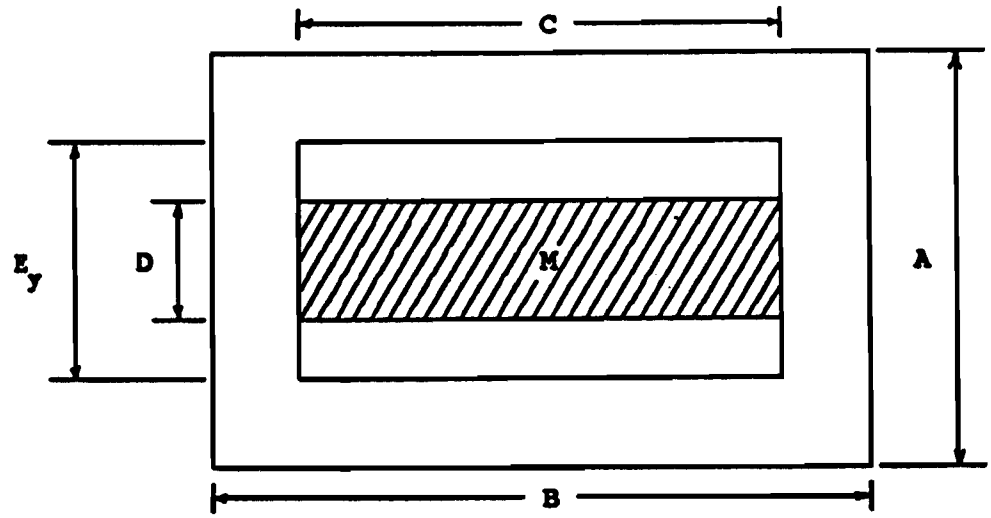

FIGURE 2 - CROSS SECTION A-A OF THE IMPACT DAMPED CLASSICAL ELASTIC CANTILEVER BEAM.

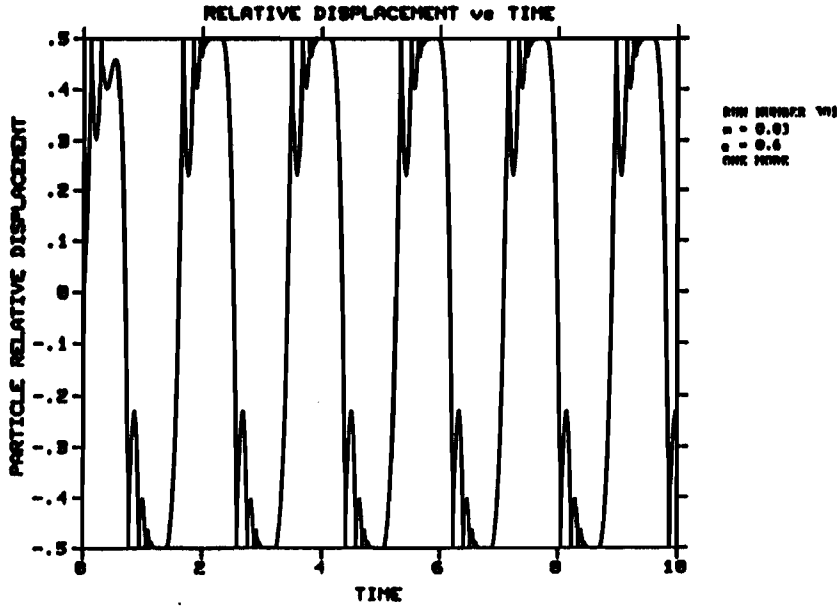

FIGURE 3 - RELATIVE IMPACTOR DISPLACEMENT OF AN INFINITE NUMBER OF IMPACTS EACH HALF CYCLE; m = 0.03; e = 0.6; ONE MODE.

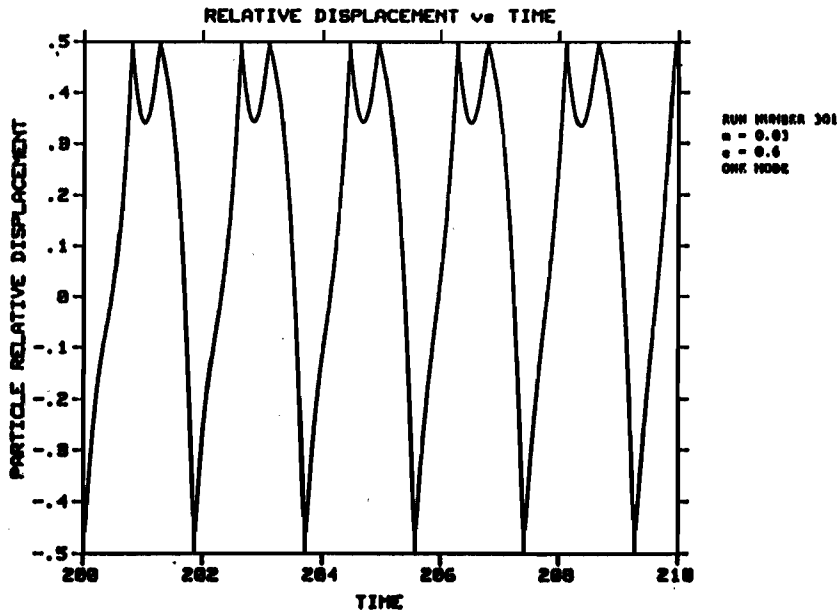

FIGURE 4 - RELATIVE IMPACTOR DISPLACEMENT OF ONE IMPACT PER HALF CYCLE ALTERNATING WITH TWO; m = 0.03; e = 0.6; ONE MODE.

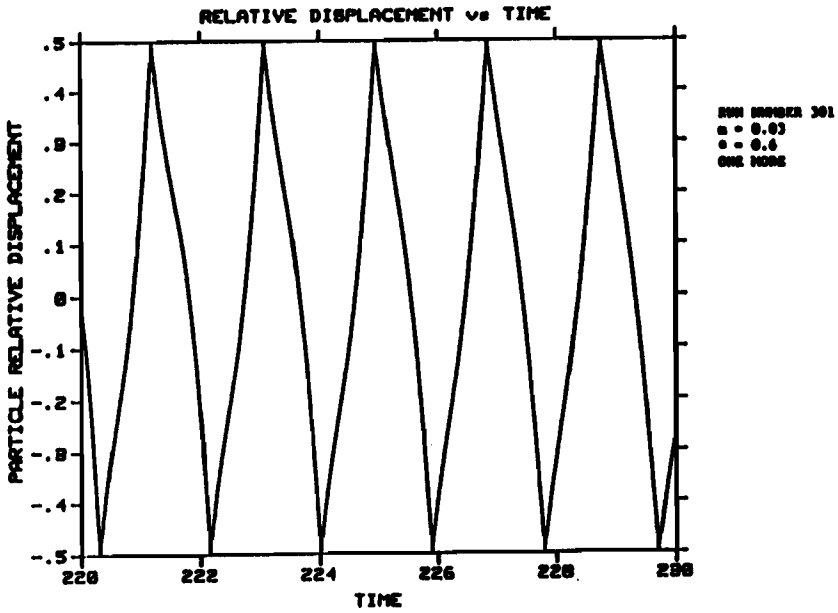

FIGURE 5 - RELATIVE IMPACTOR DISPLACEMENT OF ONE IMPACT EACH HALF CYCLE: m = 0.03; e = 0.6; ONE MODE.

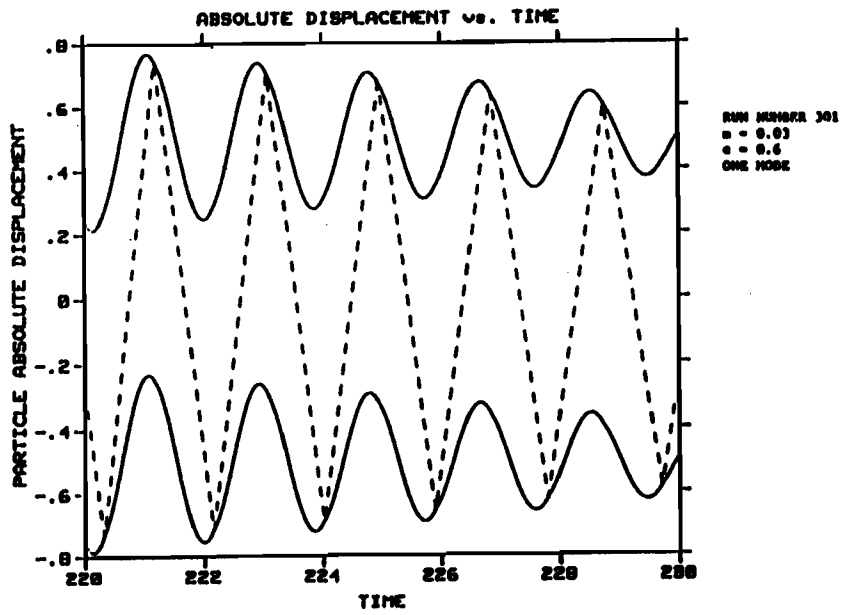

FIGURE 6 - ABSOLUTE IMPACTOR AND CAVITY DISPLACEMENT OF ONE IMPACT EACH HALF CYCLE; m = 0.03; e = 0.6; ONE MODE.

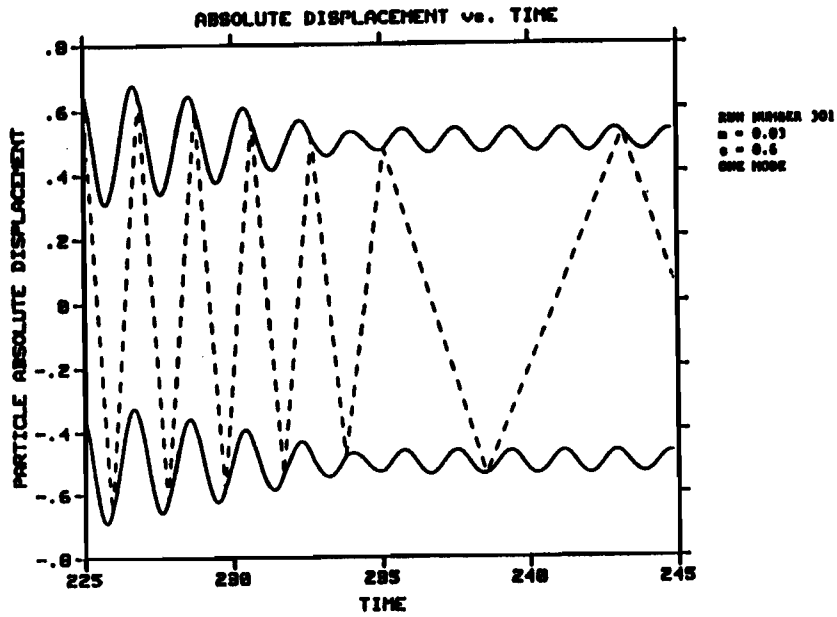

FIGURE 7 - ABSOLUTE IMPACTOR DISPLACEMENT AT THE BEGINNING OF "IMPACT DAMPER FAILURE"; m = 0.03; e = 0.6; ONE MODE.

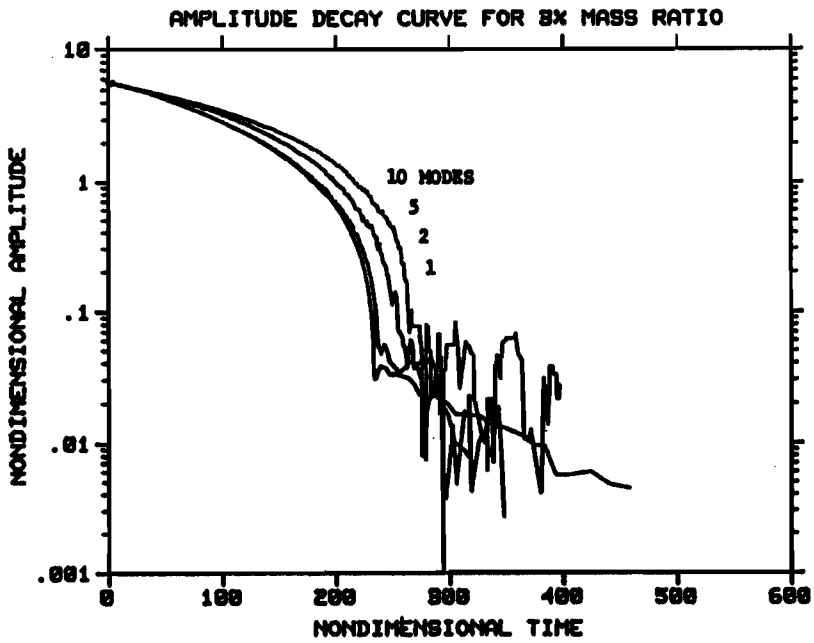

FIGURE 8 - AMPLITUDE DECAY; m = 0.03; e = 0.6; 10, 5, 2, AND 1 MODE.

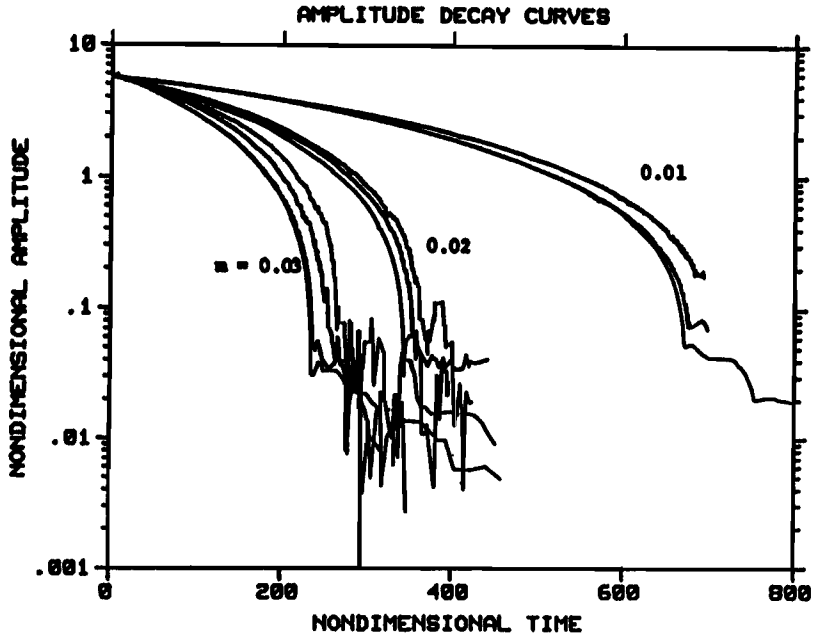

FIGURE 9 - AMPLITUDE DECAY; m = 0.03,0.02,0.01; e = 0.6; 10, 5, 2, AND 1 MODE.

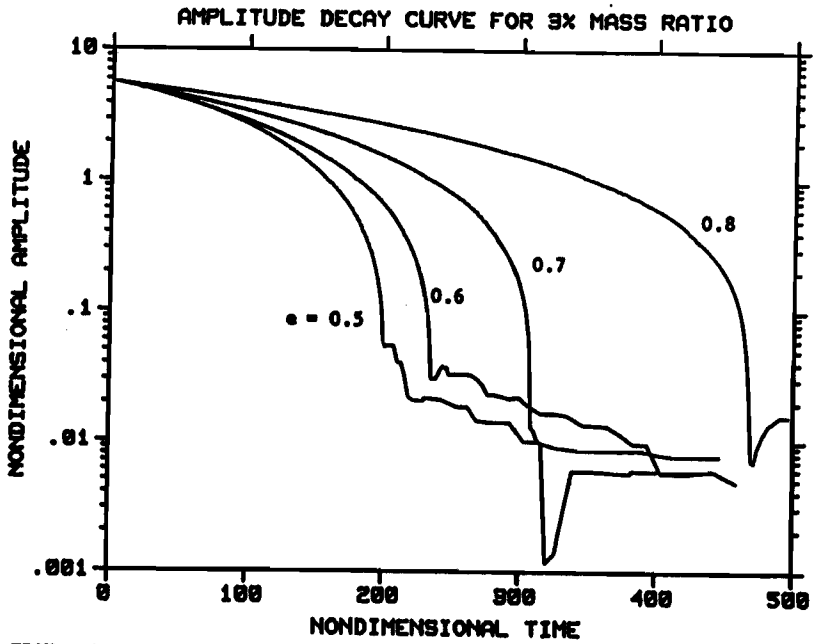

FIGURE 10 - AMPLITUDE DECAY; m = 0.03; e = 0.5 ,0.6,0.7,0.8; ONE MODE.

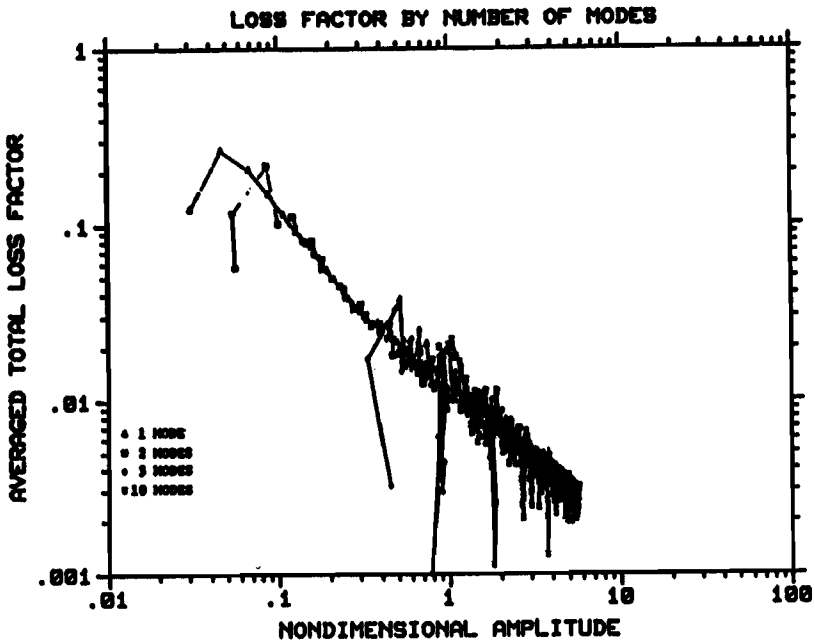

FIGURE 11 - AVERAGE TOTAL LOSS FACTOR; m = 0.03; e = 0.6; 10,5,2,1 MODE.

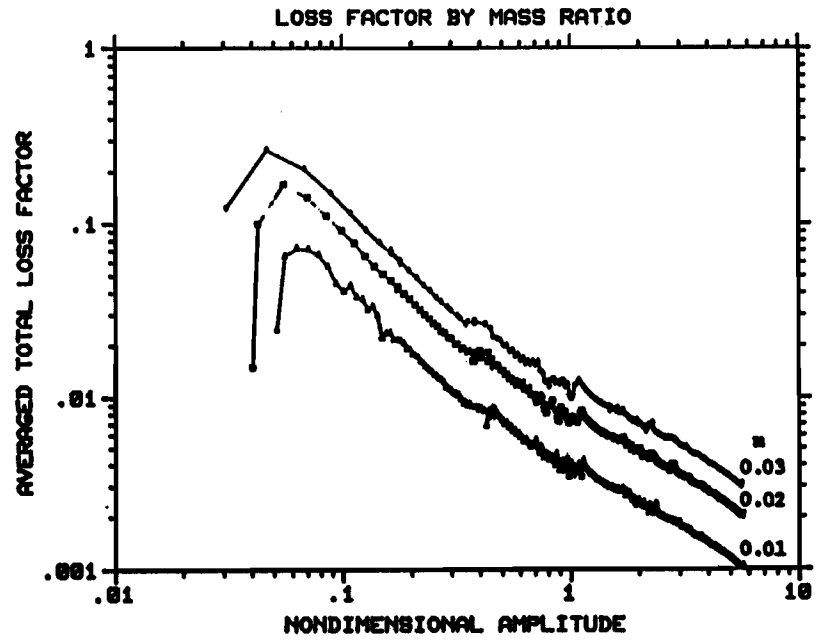

FIGURE 12 - AVERAGE TOTAL LOSS FACTOR; m = 0.03,0.02,0.01; e = 0.6; ONE MODE.

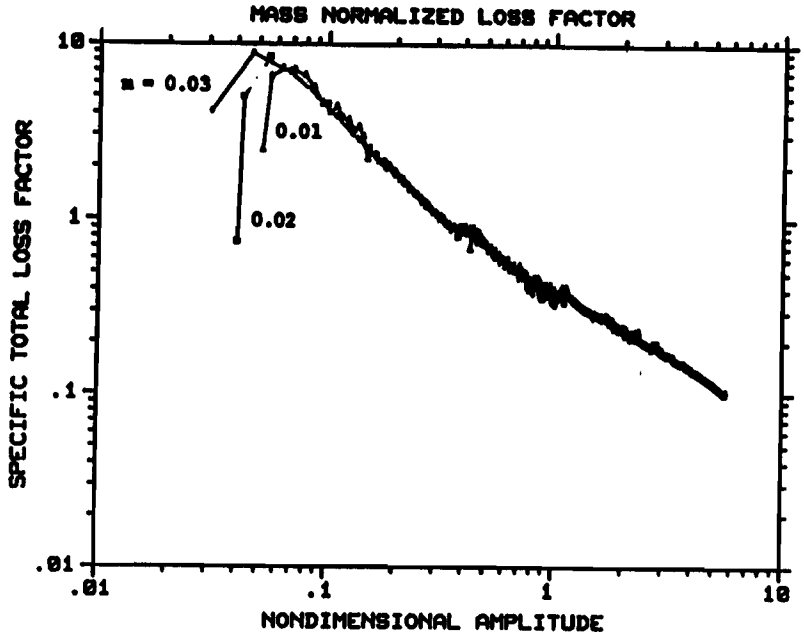

FIGURE 13 - SPECIFIC TOTAL LOSS FACTOR; m = 0.03,0.02,0.01; e = 0.6; ONE MODE.

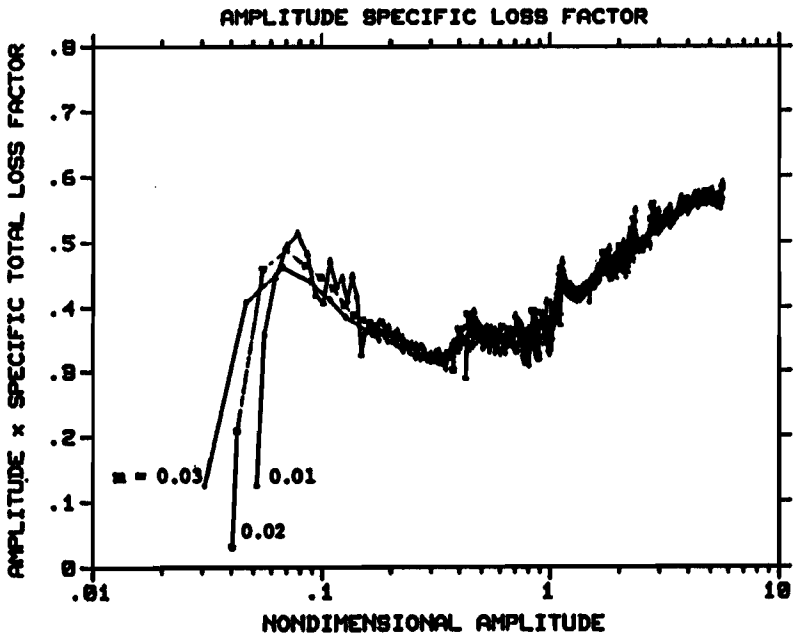

FIGURE 14 - AMPLITUDE AND SPECIFIC IMPACTOR LOSS FACTOR PRODUCT; m = 0.03, 0.02,0.01; e = 0.6; ONE MODE.

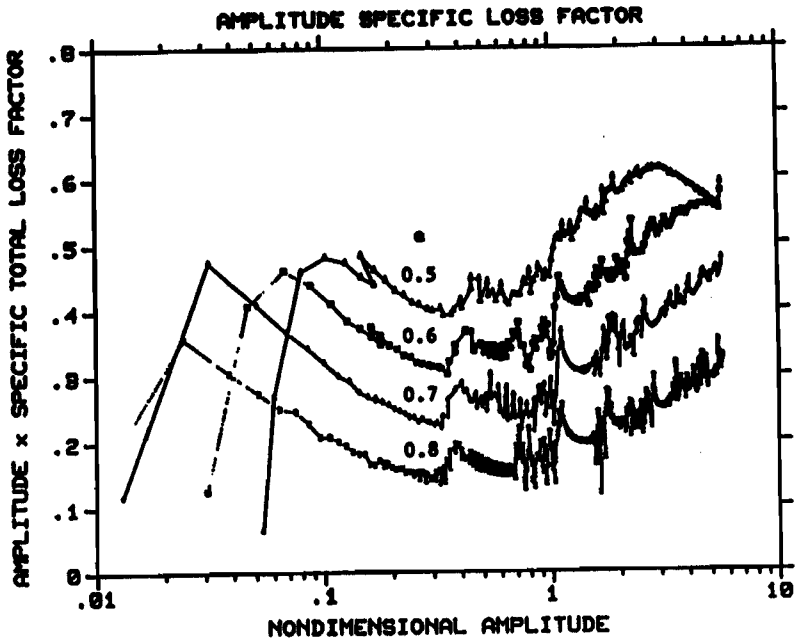

FIGURE 15 - AMPLITUDE AND SPECIFIC IMPACTOR LOSS FACTOR PRODUCT; m = 0.03; e = 0.5,0.6,0.7,0.8; ONE MODE.

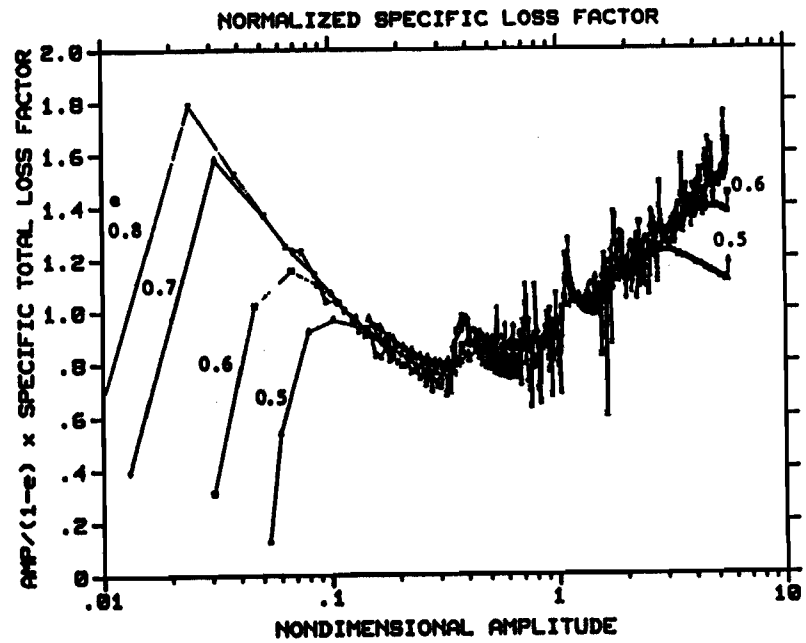

FIGURE 16 - NORMALIZED AMPLITUDE SPECIFIC LOSS FACTOR; m = 0.03; e = 0.5,0.6,0.7,0.8; ONE MODE.

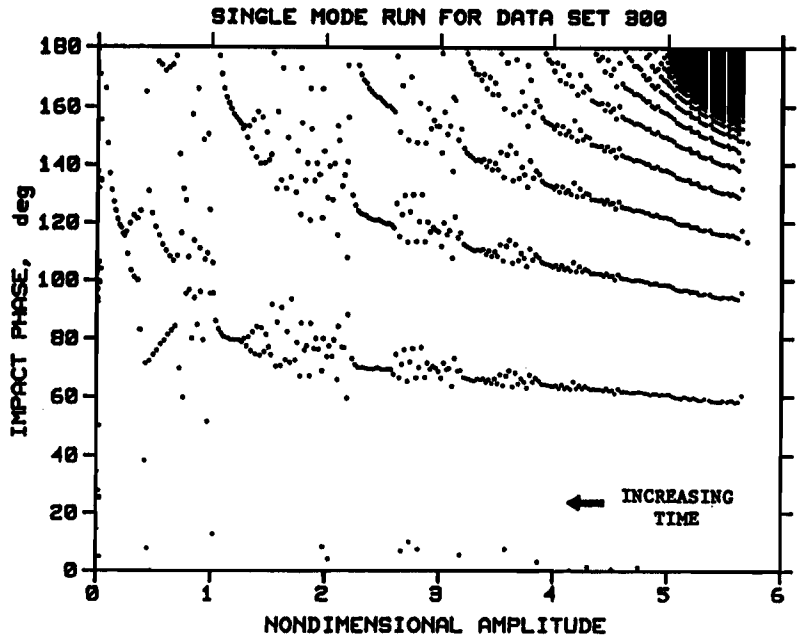

FIGURE 17 - IMPACTOR PHASE MEASURED FROM ZERO CROSSING; m = 0.03; e = 0.6; ONE MODE.

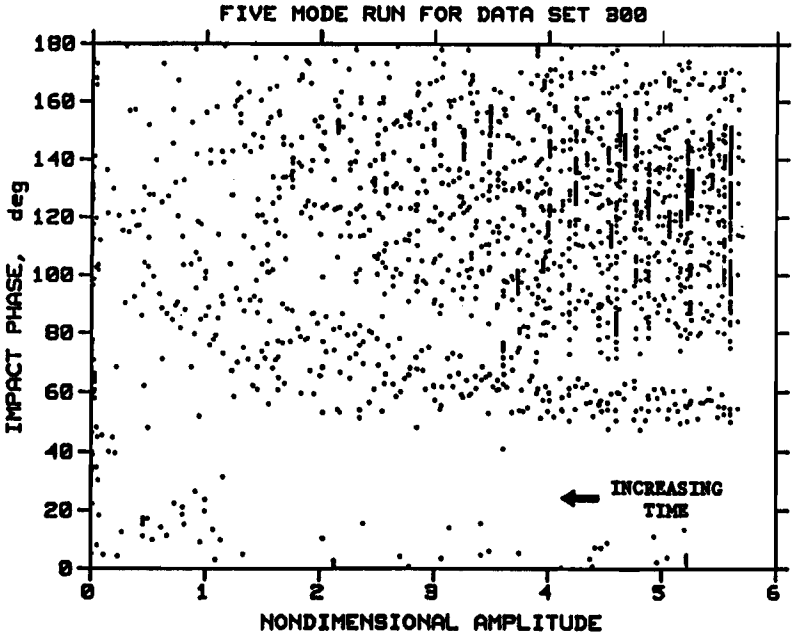

FIGURE 18 - IMPACTOR PHASE MEASURED FROM ZERO CROSSING; m = 0.03; e = 0.6; FIVE MODES.

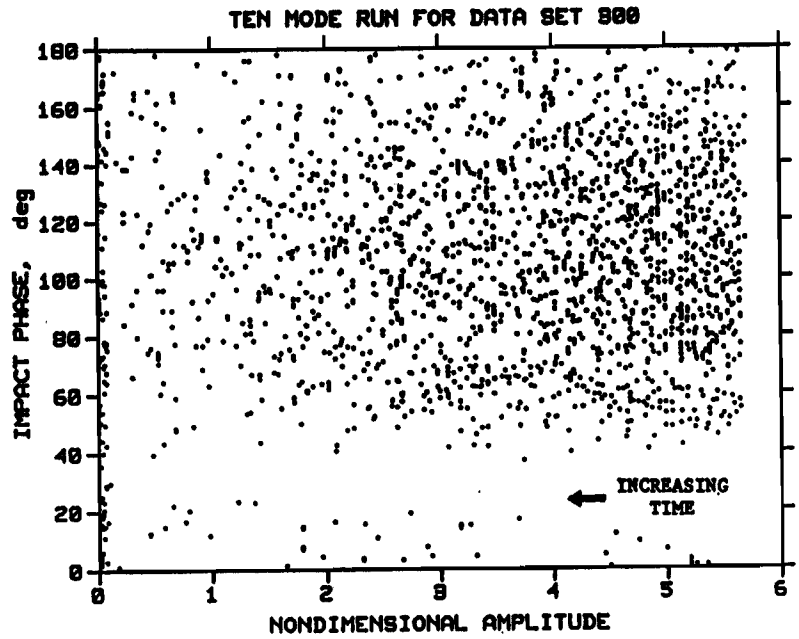

FIGURE 19 - IMPACTOR PHASE MEASURED FROM ZERO CROSSING; m = 0.03; e = 0.6; TEN MODES.

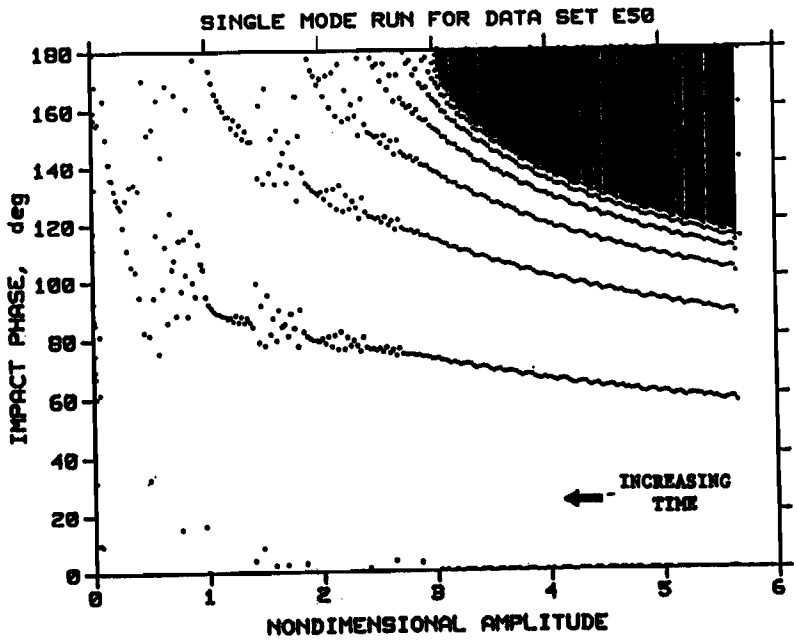

FIGURE 20 - IMPACTOR PHASE; m = 0.03; e = 0.5; ONE MODE.

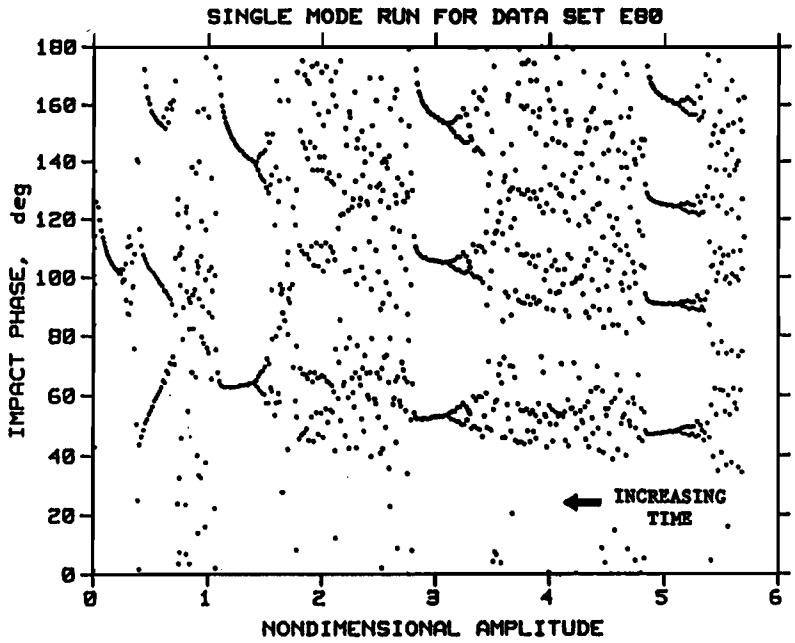

FIGURE 21 - IMPACTOR PHASE; m = 0.03, e = 0.8; ONE MODE.